IJST (2011) A1: 39-51
Iranian Journal of Science & Technology

http://www.shirazu.ac.ir/en

Multifractal analysis of the spatial distribution of earthquake epicenters in the Zagros and Alborz-Kopeh Dagh regions of Iran

A. Zamani[1]* and M. Agh-Atabai[2]

[1]*Department of Earth Sciences, College of Sciences, Shiraz University, Shiraz, Iran*
[2]*Department of Earth Sciences, College of Sciences, Golestan University, Gorgan, Iran*
E-mail: zamani_a_geol@yahoo.com

Abstract

This paper shows how multifractal analysis can be used to characterize the spatial distribution of epicenters in the Zagros and Alborz-Kopeh Dagh regions of Iran. The main multifractal characteristics, D_q, $f(\alpha_q)$, τ_q, α_q and a set of multifractal parameters defined from the shape of the $f(\alpha_q)$-spectrum including the width of $f(\alpha_q)$-spectrum, non-uniformity factor, combined parameter, coefficients of steepness and asymmetry, and vertex of the $\tau(q)$-spectrum have been determined. The results show that, in comparison with the Alborz-Kopeh Dagh region the epicentral distribution in the Zagros has a weak multifractal (i.e. less heterogeneous) structure. Although the $f(\alpha_q)$ spectra of both regions were skewed, the directions of skewing were different. The two distinct multifractal distribution patterns in these regions reflect different underlying seismotectonic processes related to earthquake activity. The diffused seismicity with fewer larger earthquakes relative to smaller ones in the Zagros and relatively low level of discontinuous seismicity with sporadic occurrence of strong destructive events in the Alborz-Kopeh Dagh confirm our findings. The results further suggest that multifractal analysis provides us with a deep insight into the complex nature of distribution and geometry associated with earthquake-related phenomena that could not be discovered by any other means.

Keywords: Iran; Zagros; Alborz; Kopeh-Dagh; multifractal; tectonics; earthquake; seismicity; seismotectonics

1. Introduction

Within the framework of the theory of complexity, the seismic phenomenon has been recognized as a chaotic self-organized critical process that obeys the scale-invariance fractal statistics. Therefore, the critical state does not require the fine tuning of some global state variables for its activation. Instabilities take place as soon as a local threshold is reached, and a cooperative phenomenon develops, spreading over all scales.

According to [1] and [2], the crust of the earth has been set up in a highly complex self-organized critical state in which the criticality manifests itself in many different geological phenomena with power-law fractal distribution and dynamics. As a specific example, seismicity patterns appear to be complex and chaotic, yet there is order in the complexity.

Numerous evidence exists that the clustering of regional seismicity appears to have a fractal-like structure [3, 4]. Multifractal analysis has provided us with a deep insight into the chaotic nature of distributions and geometry associated with earthquake clustering phenomena ([2, 5-16]).

*Corresponding author
Received: 25 April 2010 / Accepted: 30 August 2010

The well known Gutenberg-Richter formula [17] also implies a power law relation between the energy release and the frequency of occurrence of earthquake. It means that the size of the distribution of earthquakes is scale invariant and b-value has been suggested as a generalized fractal dimension of earthquake magnitude [18]. It seems that deterministic chaos provides a coordinated interpretation of the features of seismicity, which have hitherto appeared unrelated.

The spatial fluctuation in the value of fractal dimension has recently become an important theme for quantitative analysis of seismicity in active tectonic regions. Simple or homogeneous fractal models of earthquakes have been quantitatively characterized using the idea of box-counting method that corresponds in a unique fashion to the geometrical shape of the earthquake distribution patterns ([18-20, 4, 21]). In comparison with the usual box dimension, the multifractal dimensions quantify not only the fractal geometry of earthquake distribution, but also the complex geodynamic processes which take place in seismotectonic regions ([22, 23, 7, 24-27]).

Since geodynamic processes of stress accumulation and interactions between fault segments are the main sources of complexity in the

seismicity patterns of active tectonic regions, quantitative analysis of seismicity can help to reveal the nature of the seismotectonic regime of these regions. It is clear that a complete description of the fractal character of seismological data requires more than one dimension or scaling exponent, and these may also change at different locations or scales [28]. The variability of the multifractal dimensions in different seismogenic zones may be related to geologic and seismotectonic heterogeneity in these regions [29].

The conventional seismotectonic classifications of Iran were broadly defined, with considerable differences in the scheme of classification. Furthermore, the detailed data available remain limited to very restricted regions, and even the descriptive stage in this accumulation of information is incomplete. The goal of this paper, an extension of [30, 31], is the collection of numerical data to improve and refine our new approach for the construction of automated self-organized multivariate tectonic zoning maps [32]. For this purpose multifractal characteristics of the spatial distribution of earthquakes in the Zagros and Alborz-Kopeh Dagh regions of Iran (Fig.1) were analyzed using the fixed mass method [33, 34].

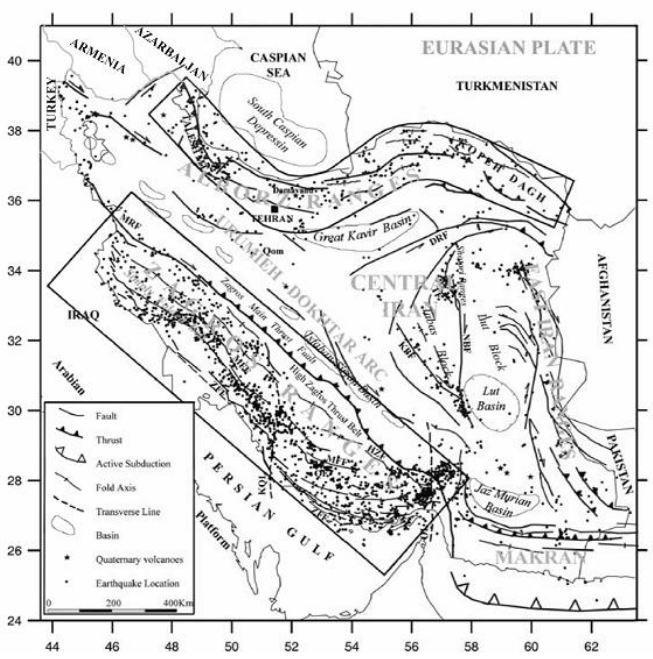

Fig. 1. Simplified seismotectonic map of Iran. DRF: Doruneh Fault, HZF: High Zagros Fault, KBF: Kuh-e-Banan Fault, KQL: Kazerun-Qatar Line, MFF: Mountain Front Fault, MRF: Main Recent Fault, NBF: Nayband Fault, OL: Oman Line, ZFF: Zagros Frontal Fault. The boxes outline the regions in which the spatial distribution of earthquake epicenters will be discussed.

2. Seismotectonic setting

The Zagros Fold-Thrust Belt of Southwestern Iran (Fig. 1) is a conformable sedimentary sequence several thousand meters thick, ranging in age from Cambrian to late Tertiary, and folded only by the late Alpine movements in Plio-Pleistocene times. These are neither metamorphic nor igneous rocks, and structures are characterized by long, parallel, asymmetric folds which form a linear inter-continental belt about 1200 km long, trending NW-SE between the Arabian shield and Central Iran, with a width varying between 200 and 300 km [35, 36]. This orogenic belt represents one of the youngest and most active seismogenic zones currently shortening and thickening due to the continued convergence between the Arabian and Eurasian plates. Three major thrust fault zones (fronts), known as the High Zagros Fault, the Mountain Front Fault, and the Zagros Frontal Fault zones, form the main tectonic framework of the Zagros Fold-Thrust Belt (Fig. 1). Between them, run a series of transfer fault zones oblique to the belt [37]. The High Zagros Fault zone divides the Zagros into two major parallel structural zones known as the Imbericated or High Zagros Thrust Belt (an intensely deformed zone) to the northeast and the Simply Folded Belt to the southwest. The Mountain Front Fault zone which comprises sets of active reverse faults coincides with the 1500 m contour and the seismic activity is mainly concentrated along these frontal active faults to the southwest of the Simply Folded Belt. The Zagros Fold-Thrust Belt is sharply delineated along its southwestern border by the Zagros Frontal Fault

zone, also called the Zagros Foredeep Fault zone. It separates the Zagros alluvial basin to the southwest from the mobile fold-thrust mountain belt to the northeast [37-40]. The most striking feature of the seismicity of the Zagros is an abrupt cut-off of activity in the NE, along the Main Zagros Thrust Fault (Fig. 1). Except in the NW of the Zagros belt, where the boundary of seismicity coincides with the Main Zagros Thrust Fault, most of the larger earthquakes ($m_b \geq 5.0$) in the Zagros occur along its SW front, between the coast of the Persian Gulf and the Mountain Front Fault. In the southeastern Zagros, seismicity is distributed in a curvilinear band, and there is a notable absence of seismicity between this band and the Main Zagros Thrust Fault [36, 41]. The pattern of seismicity in the Zagros region is diffused. On the whole, major earthquakes in this region are not common and careful studies of earthquake locations have failed to reveal activity deeper than about 25 km [42]. Moreover, past earthquake activity suggests that the seismicity of this region has been continuous with occasional local paroxysms .

The Alborz-Kopeh Dagh is one of the major earthquake belts of Iran [43], extending for a distance of about 1500 km and with a width varying between 60 and 120 km. The Alborz Mountain constitutes a broad arch of parallel folds extending from north to northeast Iran separating the Caspian low land from the Iranian Plateau and merging with the Kopeh Dagh Mountains toward the east (Fig. 1). The region is characterized by several episodes of regional metamorphism and magmatism during the Paleozoic and Mesozoic times. Tectonic movements were renewed in the Plio-Pleistocene phase of the Alpine orogeny. According to [35] and [36] the central Alborz range has a crustal thickness of ~35km, with a structure typical of continents. The isolated and prominent volcano of Damavand, with its alkaline activity continuing into Holocene times, seems to be related to the subduction of the central Caspian beneath the coast in the Alborz region [44-49]. The Kopeh Dagh is an active fold belt formed on the southern margin of the Eurasian plate separating the Turkmenistan (Turan) shield from central Iran; it is the northeastern border of the Iranian Plateau. Like the Zagros belt, the sedimentary cover was folded into long linear NW-SE folds perpendicular to the trend of the relative motion of the Arabian and Eurasian plates. This fold-thrust belt is up to 3000 m in elevation, rising 2000 m above the Turkmen plains [43]. Earthquakes in the Kopeh Dagh involve mostly right-lateral strike-slip faulting trending N to NNW or reverse faulting parallel to the NW regional strike [50-51, 44, 36]. The abrupt linear topographic front forming the NE margin of the Kopeh Dagh follows a fault zone referred to as the Main Kopeh Dagh or Ashkabad Fault. This fault zone was associated with a large (M_s 7.2) earthquake in 1948, the focal mechanism of which remains uncertain (e.g. [52], [36]) and where the co-seismic surface ruptures were ambiguous [50], [53]. The pattern of seismicity in the Alborz-Kopeh Dagh region is discontinuous, but with gaps filled in gradually by relatively large events. The belt is characterized by a high proportion of large magnitude shallow earthquakes. [54], [36.[

The global earthquake catalogues used in this research were compiled from the bulletins of the International Seismological Center [55] and the US. Geological Survey Preliminary Determination of Epicenters [56] for the period January 1964 up to the end of September 2008, which comprises over 4000 events for the Zagros and 700 events for the Alborz-Kopeh Dagh regions. Since in many works (e.g. [43]) the Alborz and Kopeh Dagh mountain ranges have been considered as a single earthquake belt, in this research the borders of the Alborz ranges were extended to cover the Kopeh Dagh ranges as well. The borders of the examined regions have been delineated in Fig.1 [57]. The magnitude of completeness, M_c, with 90% confidence level is equal to 4.5 for the Zagros and 4.4 for the Alborz-Kopeh Dagh regions, respectively [36], [58]. After eliminating all the events having magnitudes less than M_c, the b-value of the [17] magnitude-frequency relation has been estimated using the weighted least square method [59]. The estimated b-values for the Zagros and Alborz-Kopeh Dagh regions are 1.47±0.03 and 1.29±0.02, respectively [30]. To guarantee the completeness of data, analysis will comprise only events with magnitudes equal to or larger than Mc. In the case of events with $m_b \geq M_c$, there was an improvement in epicentral locations as more instruments were added to the worldwide network of seismological stations [60, 42]. According to [60] and [61] earthquakes larger than about $m_b \geq 4.4$ have locations accurate to about 15-20km comparable with location errors of the global earthquake catalogues [62], [12].

3. Data analysis

The concept of fractal provides a means of testing whether earthquake distribution is a scale-invariant process or not. Earthquake occurrence as a critical phenomenon appears to be multifractal and chaotic. Multifractal analysis is a useful tool for showing patterns in the complex nature of distributions and geometry associated with earthquake activity that could not be revealed by any other means. There are many fractal measures to quantify the geometry of complex or chaotic behavior of earthquake distribution. The Rényi or generalized correlation

dimensions D_q, also known as the spectrum D_q of dimensions (with q ranging from -∞ to +∞), defines the probabilistic distributions of multifractal phenomena such as earthquake distributions. Another equivalent way to describe multifractal distributions is the so-called $f(\alpha_q)$-spectrum, also known as the singularity or Legendre spectrum [63], [30].

Suppose we cover the support of our distribution with N spheres of radius r, centered on N randomly chosen reference points and define $P_i(r)$ to be the distribution probability of epicenters in the ith (i=1, 2, …, N) sphere.

$$P_i(r) \approx r^{-\alpha_i} \tag{1}$$

Where α_i is singularity strength or Lipschitz-Hölder exponent, also known as the crowding index of the probability subset α which corresponds to the fractal dimension at i point and varies from place to place. If all spheres have the same scaling with the same α_q (i.e. α_q is independent of the location of the event), the distribution is homogeneous or monofractal [64]. For estimating D_q, at first the so-called partition function (because of analogies with the partition function in the theory of equilibrium thermodynamics) should be determined [65-67].

$$Z(r,q) = \sum_{i=1}^{N} \{P_i(r)\}^q \tag{2}$$

The exponent q is a real number which indicates the order of the moment of the probability $P_i(r)$. It plays an important role in the characterization of a multifractal distribution by enhancing the smallest differences between two apparently similar distributions [68]. High values of q enhance spheres with relatively high values for $P_i(r)$, while low values of q favor spheres with relatively low values of $P_i(r)$. Therefore, by selecting appropriate values for r and q, the partition function Z (r, q) furnishes information about multifractal distributions at different scales and moments. The generalized multifractal dimensions D_q is defined:

$$D_q = \frac{1}{q-1} \lim_{r \to 0} \frac{\log Z(r,q)}{\log r} \tag{3}$$

The graph of D_q as a function of q is constant and equals the topological dimension where Euclidean sets were considered. If epicentral distribution is homogeneous or monofractal (i.e. it has no structure), D_q assumes the same value for all q values (i.e. $D_0=D_1=D_2=\ldots=D_{+\infty}$).

In this case the D_q curve becomes a straight line through D_0 parallel to the abscissa, otherwise D_q decreases monotonically with q for the inhomogeneous or multifractal distribution (i.e. $D_0>D_1>D_2>\ldots>D_{+\infty}$) [30]. For q=0 the common capacity dimension D_0, for q=1 the information dimension D_1, and for q=2 the correlation dimension D_2 were obtained. $D_{+\infty}$ and $D_{-\infty}$ are the lower and upper limits of multifractal dimensions and give information about the most intense and the least intense clustering of the seismicity (i.e. where $P_i(r)$ is larger and smaller, respectively). For multifractal distribution, the rate of decrease (slope) may remain the same or change from one pattern to another. The high rate of decrease corresponds to a steep type of D_q spectrum and the low rate corresponds to a gentle type of D_q spectrum. That is, the slope of D_q spectrum becomes gentle for extended distribution of earthquakes and steep for clustered distribution of earthquakes. Since D_q for negative q can take a value larger than the spatial dimension d, calling D_q a dimension makes no geometric sense when D_q >d [34], [69]. If the limits in (3) cannot be calculated because of insufficient information at small scales or due to lack of scaling below a minimum physical length, a scaling region in the partition function can be found that behaves as

$$Z(r,q) \approx r^{\tau_{(q)}} \tag{4}$$

where, the partition function exponent τ_q is called the q_{th}-order correlation exponent or the sequence of the mass exponent. The slope τ_q of the power-law fitted to the scaling region is related to D_q by

$$\tau_{(q)} = (q-1)D(q) \tag{5}$$

the effect of the normalization is that τ_q=1=0 and τ_q=0=D_0 because for q=0, the partition function is just the count of spheres needed to cover the distribution [30]. If $N_\alpha(r)$ is the cardinality of a subset formed by the spheres in which the probability $P_i(r)$ has the same singularity strength α_q, for a multifractal distribution

$$N_\alpha(r) \approx r^{-f(\alpha_q)} \tag{6}$$

$f(\alpha_q)$ is, so to speak , a fractal of fractals and quantifies the irregularities in the seismicity pattern from the neighborhood of one event to the neighborhood of another [63], [27]. Thus, it is the fractal dimension of the subset in which α_i equals α**.**

D_q is linked to $f(\alpha_q)$ by

$$D_q = \frac{1}{q-1}\left[q\alpha(q) - f(\alpha(q))\right] \tag{7}$$

which is derived from (3) by the gradient method or method of steepest descent [70], [71], [67], [72].

α_q and $f(\alpha_q)$ are related to q and $\tau(q)$ by

$$\alpha(q) = \frac{d\tau(q)}{dq} \tag{8}$$

$$f(\alpha(q)) = q\alpha(q) - \tau(q) \tag{9}$$

equations (8) and (9) constitute a so called Legendre transformation from the independent variables τ and q to the independent variables f and α and the functions $f(\alpha_q)$ in (9) and τ_q in (5) are Legendre transforms of each other [73]. One can identify $\sum_i \{P_i(r)\}^q$, τ_q, $f(\alpha_q)$, α_q, and q with the "partition function", "free energy", "entropy", "internal energy", and "inverse temperature" in thermodynamics, respectively [74], [67]. The $f(\alpha_q)$-spectrum, which represents a description of multifractals equivalent to D_q, has several interesting properties. First, standard properties of the Legendre transform (9) with (8) imply that the graph of $f(\alpha_q)$ has a parabolic form (i.e. quadratic expression), that concaves upward, peaks at (f_{max}, α_q =0), and stretches from α_{min} to α_{max} where $f_{max}=D_0$, α (f_{max})= α_q =0=α_0, and α_{min} and α_{max} satisfy $f(\alpha_q)$=0 [64], [30]. Most earthquake epicenters contribute to the peak because it is the highest fractal dimension present in the union of the interwind fractals of different dimensions and the related α_q is denoted as α_0. The low and large sides of the spectrum correspond to the concentrated and rarified regions of epicentral locations, respectively. The decrease of $f(\alpha_q)$ function on both sides of the spectrum indicates that there are fewer regions with relatively high and low concentrations of epicenters in the union. The range α_{min} to α_{max} quantifies the heterogeneity of the multifractal structure, while $f(\alpha_q)$ indicates how frequently events with scaling exponent α occur in the set. In addition, (9) shows that $\frac{df(\alpha_q)}{d\alpha_q} = q$.

Thus, the slope of $f(\alpha_q)$ is given by the order q of the moment related to α_q. The maximum of $f(\alpha_q)$ occurs for α_q =0 and is equal to D_0. Also from eq. (7) with q=1, it is found that $f(\alpha_q)$= α_q =D_1, thus the slope $\frac{df(\alpha_q)}{d\alpha_q}$ there is unity.

The subset for q<0 corresponds to that with $\alpha_q > \alpha_0$, and the smaller the q, the larger the α_q. The subset for q>0 corresponds to that with $\alpha_q < \alpha_0$, and the larger the q, the smaller the α_q. To get a complete multifractal spectrum, q should range from -∞ (α_{min}) to +∞ (α_{max}). Thus, the large α_q side ($\alpha_q > \alpha_0$) is generated by earthquake epicenters in sparsely populated regions. The low α_q side ($\alpha_q < \alpha 0$) describes densely clustered earthquake epicenters. The lower value of $f(\alpha_q)$, i.e. the lower fractal dimension of the epicentral distribution, shows that there are fewer epicenters [64], [30].

In this study the fixed-mass technique (10) was used because D_q for negative q, which characterizes the multifractal measures of seismic gap areas is as important as D_q for positive q, which characterizes the earthquake activity in cluster regions. This technique also provides greater reliability and sensitivity to small changes in clustering properties of multifractal phenomena [33, 34].

$$\log\left\langle R_i(<m)^{-\tau(q)}\right\rangle^{1/\tau_q} \approx \log m^{-1/D_q} \tag{10}$$

Where, R stands for radius, m for the number of points in the vicinity of a given point i, τ_q is a real number related to D_q through (5), and < > means the average for radius. In this technique the distribution of earthquake epicenters is covered with spheres of different radii, but all containing the same mass, m. We then obtain how the smallest radius R_i (<m), within which a fixed-mass m is included, increases as the mass increases [34], [22].

The multifractal analysis is performed using the software toolbox designed for the nonlinear analysis of earthquake distribution written under Matlab and Zmap [22], [59], [75].

4. Results

In the procedure for estimating D_q spectra as a function of q for the epicentral distribution of earthquakes in the Zagros and Alborz-Kopeh Dagh regions, the correlation integral functions $\left(\left\langle R_q \right\rangle\right)$ for different values of τ have been calculated. In calculating D_q we chose a large range of $\tau_{(q)}$, varying between -4.0 and 4.0 to accommodate q values in the range -10 to 10, with special interest in values of q close to 0 and 2. The appearance of high frequency oscillations for small negative values of q makes it difficult to estimate D_q. Furthermore, discreteness effects and lack of statistics can affect the evaluation of D_q for large positive values of q [76].

For a multifractal distribution a linear relationship or a linear relationship with oscillations superimposed should be observed. From this plot we estimate the slope, which corresponds to $-1/D_q$. Then q is calculated from (5), and finally, D_q is drawn as a function of q [77]. The main contribution to D_q for large positive q is given by a subset of spatial distribution of epicenters with very high probabilities. D_q values for large negative q were determined mainly by the subsets with very low probabilities. The values of D_q for the epicentral distribution of earthquakes in the Zagros and Alborz-Kopeh Dagh regions of Iran were measured according to Equation (10), α_q from (8),

and finally, utilizing α_q in (9), $f(\alpha_q)$ was obtained. For negative q, the multifractal spectra $f(\alpha_q)$ is more sensitive to the inaccuracy of the estimates of low probabilities. Therefore, the right-hand side of $f(\alpha_q)$ ($\alpha > \alpha_0$) is less reliable than the left-hand side. $f(\alpha_q)$ and D_q, which incorporate deeper mathematical subtleties, have been successfully used for the analysis of many fractal and chaotic phenomena by many researchers [33], [23], [78], [34], [79], [26], [27]. The $\tau(q)$ versus q curve, also called $\tau(q)$-spectrum, shows the nonlinear dependence of the τ function on q. The vertex of the $\tau_{(q)}$ curve becomes narrower or wider for more heterogeneous and less heterogeneous multifractal distributions, respectively. This curve snuggles up to two unique lines of support (i.e. asymptotes) of slopes $-\alpha_{min}$ and $-\alpha_{max}$ [70], [80]. Similar to the $f(\alpha_q)$-spectrum, the $\tau_{(q)}$ is less reliable for negative values of q. Other multifractal parameters that were used as possible measures of earthquake activity in the study regions are: $\alpha_0=\alpha(f_{max})$, width of multifractal spectrum $w=(\alpha_{max}-\alpha_{min})$, non-uniformity factor $\Delta=(\alpha_{max}\_\alpha_{min})/f_{max}$, and combined parameter $P_c=[\alpha(f_{max})/f_{max}]\Delta\alpha_{1/2}$, where $\Delta\alpha_{1/2}$ is full-width-at-half-maximum [30]. The local fractal dimension α_0 related to the peak of $f(\alpha_q)$-spectrum gives an indication whether the underlying process is regular in appearance or not; i.e. the larger α_0 indicates a more regular process.

To be able to make a quantitative characterization of $f(\alpha_q)$, particularly the relative dominance of fractal exponents within the multifractal distribution, the spectrum was fitted to a quadratic function (i.e. parabolic form) around the position of its maximum at α_0.

$$f(\alpha(q)) = A(\alpha(q)-\alpha_0)^2 + B(\alpha(q)-\alpha_0) + C \quad (11)$$

Where A, B, and C are parameters that can be determined by ordinary least-squares procedure. The coefficient A is the steepness parameter; changing A broadens or narrows the spectrum. The coefficient B serves as an asymmetry parameter, which is zero for symmetric shapes, and positive or negative for a right-or left-skewed (centered) shape, respectively. In this procedure the additive constant $C=f(\alpha_0)=1$ [81], [27], [30].

In this paper we measure the pairwise distances between epicenters, thus only relative errors influence the results. In order to estimate the uncertainty of the multifractal parameters, the same analysis was performed on a limited number of reference points selected randomly among the data points [34]. For this purpose one third of the data points of each study region were chosen as reference points by using 10 different sequences of random numbers. Although the scatter estimation error is large for negative q, the uncertainty is small for positive q. The scatter of these estimates indicates the errors in estimating the multifractal parameters (Table 1). The results verify that the variability of the multifractal parameters is not random, but statistically significant.

4.1. Multifractal properties of the Zagros epicenters

More than 50% of teleseismic recorded earthquakes in Iran have occurred in the Zagros region, but their magnitudes are all less than M_w 7.0. with the exception of the NW of the Zagros belt, where the boundary of seismicity coincides with the Main Recent Fault, most of the larger earthquakes in the Zagros occur along the Mountain Front Fault. Smaller earthquakes occur throughout the region [38], [36], [41], [82]. Nearly all earthquakes in the Zagros region occur in the upper crust with a median depth of 15±7 km [35].

The generalized correlation integral functions $\left(\left\langle R_q \right\rangle\right)$ for the epicentral distribution of earthquakes with magnitude $m_b \geq$ (M_c=4.5) in the Zagros region were calculated and plotted on double logarithmic coordinates (Fig.2).

The correlation integral functions were fitted to a straight line. The self-similarity behavior of the epicentral distribution of earthquakes can be observed at m_{min}=10 to m_{max}= 160, corresponding roughly to a distance range of 20 - 100km, respectively. For small distances the generalized correlation integral was influenced by location error and the "depopulation" effect [62], [12], [83], [84].

As for the upper boundary of the scaling range, there are some intrinsic characteristic scales in the earthquake faulting, such as the geometry of the lithospheric plate boundary and the extent of the topographic relief and/or isostatic anomalies within the lithosphere [85].

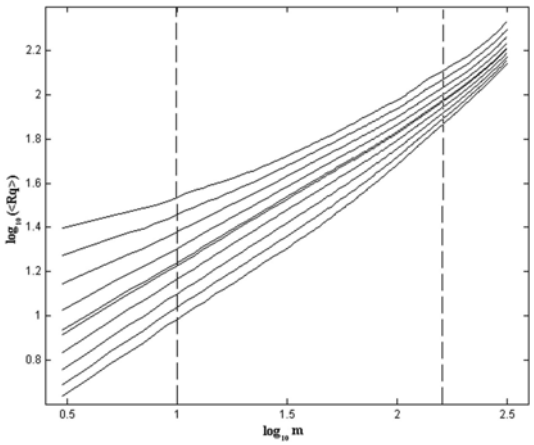

Fig. 2. The double logarithm plots of the generalized correlation integral function (τ_q = -4, -3, -2, -1, -0.1, 0.1, 1, 2, 3, 4 from top to bottom) for the spatial distribution of epicenters in the Zagros region.

The upper cut-off for the scaling range was probably generated by earthquakes that were associated with highly stressed regions containing prominent seismotectonic features such as the Kazerun-Qatar Line (KQL) and the Main Recent Fault (MRF), which according to [82] and [86] include segments of a series of fault zones with ~100km lengths. The values of D_q were obtained from the slopes of the graphs of log $\left(\left\langle R_q \right\rangle\right)$ versus log (m) and the spectra of D_q as a function of q for the epicentral distribution of earthquakes were plotted (Fig.3).

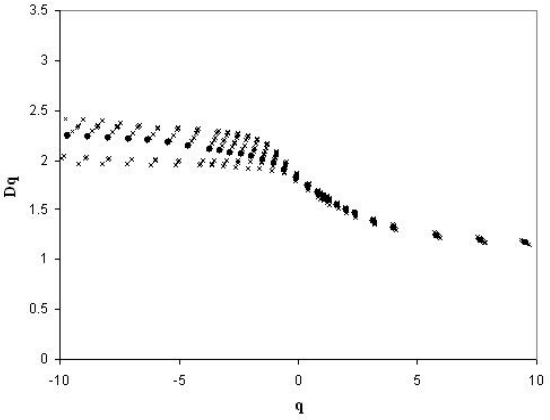

Fig. 3. The spectra of generalized fractal dimensions D_q for the spatial distribution of epicenters in the Zagros region. All data points are used as the reference points to determine the solid circles. Randomly chosen, one third of data points are used to obtain the crosses.

The maximum fractal dimensions $D_{-\infty}$ of about 2.29±0.17 and the lower limits of fractal dimensions $D_{+\infty}$ of 1.13±0.01 were obtained for the epicentral distributions of earthquakes, respectively. D_0 of about 1.83±0.03, D_1 of about 1.63±0.02, and D_2 of about 1.5±0.01 were calculated for the epicentral distribution, respectively (Table 1). It is interesting to note that the D_q spectrum has a steep slope for q>0, i.e. it saturates slowly towards $D_{+\infty}$ while the convergence to $D_{-\infty}$ is gentle (Fig.3). The latter implies that the sparsely populated regions are less heterogeneous than the densely clustered areas. This indicates an asymmetrical distribution of the multifractal structure, which results in the leaning of (i.e. left-skewed) $f(\alpha_q)$-α_q diagram (Fig. 4).

The functions D_q and $f(\alpha_q)$ are fundamental characteristics of multifractal distributions. The maximal value of $f(\alpha_q)$ is equal to D_0. The values α_{min} and α_{max} are linked correspondingly to extremal values of the spectrum of generalized fractal dimensions $D_{+\infty}$ and $D_{-\infty}$, respectively.

The value α_{min} describes the scaling in more densely populated domains, while α_{max} highlights the scaling in more sparsely populated regions (Fig.4).

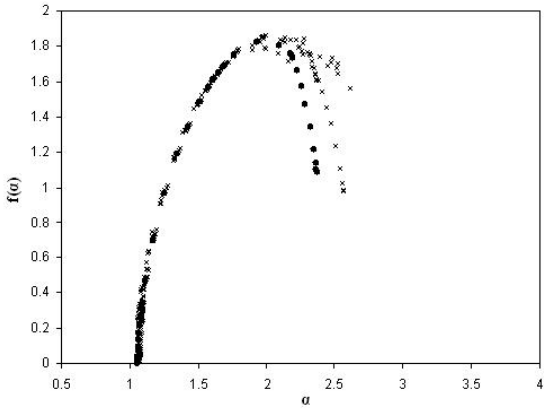

Fig. 4. The multifractal or singularity spectrum $f(\alpha_q)$ for the spatial distribution of epicenters in the Zagros region. Symbols are shown in Fig. 3.

In comparison with α_0 in the Alborz-Kopeh Dagh spectrum, the Zagros belt spectrum has a smaller α_0, indicating that the underlying process in the epicentral distribution of this belt is probably less regular (Figs. 4 and 8). The singularity spectrum $f(\alpha_q)$ quantifies the regional correlation properties of the spatial distribution of epicenters in the study region. The multifractal parameters characterizing the shape of the $f(\alpha_q)$-α_q diagrams are α_{min}, α_{max}, f_{max}, $\alpha(f_{max})$, w, Δ, P_c, A, and B. These parameters were used for quantitatively characterizing the multifractality of the spatial distribution of earthquakes that generates the seismicity pattern in the Zagros region (Table1). A value of α_0=1.92±0.06 was determined for the local fractal dimension related to the peak of $f(\alpha_q)$ spectrum. The values of w=1.7±0.29, Δ=0.93±0.16, and P_c =1.32±0.28 imply that the multifractal distribution of epicenters in the Zagros region is relatively more homogeneous than in the Alborz-Kopeh Dagh (Table 1). The parameters of steepness A=-1.38±0.04, and asymmetry B=-0.12± 0.03 show that, in contrast to the Alborz-Kopeh Dagh, the $f(\alpha_q)$ spectrum of the Zagros descends steeply and has an asymmetrical (i.e. left-skewed) shape characterized by a relative dominance of low-fractal exponents.

The $\tau_{(q)}$-spectrum for the spatial distribution of epicenters consists of a curve with a relatively wide vertex $\theta=170^{\circ}$, indicating an almost uniform (i.e. less heterogeneous) multifractal distribution of earthquake epicenters in the Zagros region (Fig. 5).

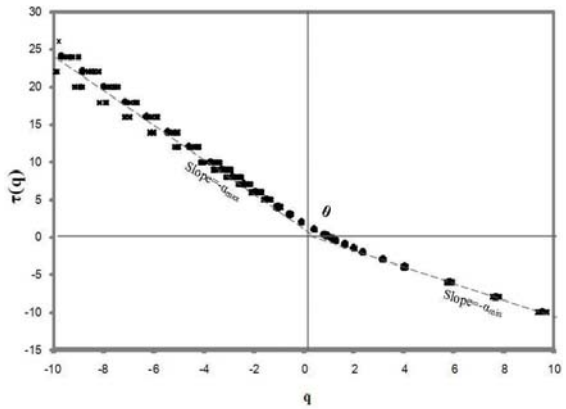

Fig. 5. The hierarchy of scaling exponents τ(q) or τ(q)-spectrum as a function of moment order q with the asymptotes (dashed lines) for the spatial distribution of epicenters in the Zagros region. In order to avoid the scatter-estimation errors for high values of q, the vertex θ is determined for the range of q between -4.0 and 4.0. Symbols are shown in Fig.3.

4.2. Multifractal properties of the Alborz-Kopeh Dagh epicenters

In contrast to the Zagros Fold-Thrust Belt in which the number of moderate size earthquakes is larger relative to the number of big events, the Alborz-Kopeh Dagh region shows a rather low level of seismicity with sporadic occurrence of large and destructive earthquakes. Although earthquakes in this region occur at all depths in the crust with a median depth of 20±8 km, seismic activity occurs primarily in the upper crust with some infrequent events to a depth of up to ~30 km. In some parts earthquakes occur generally on low angle thrust faults, indicating underthrusting of the south Caspian Sea floor beneath the NW Iran coast [35], [87].

Similar to the Zagros Fold-Thrust Belt, the plots of log $\left(\left\langle R_q \right\rangle\right)$ versus log m for the epicentral distribution of earthquakes with $m_b \geq$ (M_c=4.4) were fitted to a straight line (Fig. 6).

The scale-invariant behaviour can be observed between m=3 and m=58, which is is approximately between 20 and 130 km in distance. The edge effects associated with depopulation at small m and saturation at large m, were avoided. For small distances the gradient of log $\left(\left\langle R_q \right\rangle\right)$ versus the log (m) curve becomes artificial because of the location error and the low threshold magnitudes of earthquake catalogues. The upper cut-off for the scaling range corresponds to the width (up to 120 km) of the study area [43].

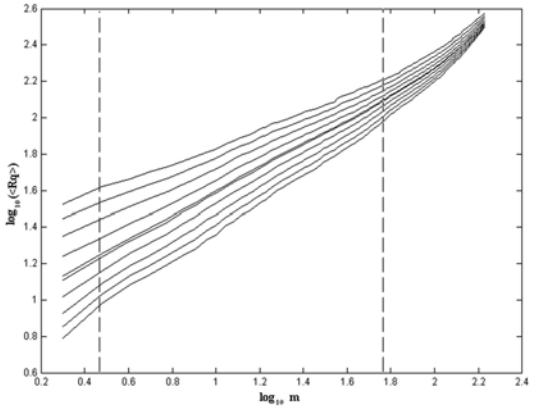

Fig. 6. The double logarithm plots of the generalized correlation integral function (τ_q = -4, -3, -2, -1, -0.1, 0.1, 1, 2, 3, 4 from top to bottom) for the spatial distribution of epicenters in the Alborz-Kopeh Dagh region.

The spectrum of D_q as a function of the moment order q for the spatial distribution of epicenters was plotted (Fig. 7).

The D_q spectrum shows that the densely clustered regions are less heterogeneous than the sparsely populated areas. This results in a markedly right-skewed (centered) f(α_q) spectrum characterized by a relative dominance of high fractal exponents within the multifractal spatial distribution of epicenters in the Alborz-Kopeh Dagh region (Fig. 8).

In comparison with the Zagros, the τ(q)-spectrum for the spatial distribution of epicenters in the

Alborz-Kopeh Dagh region consists of a curve with a relatively narrower vertex θ=160º, suggesting that the distribution of epicenters in this region has a non-uniform (i.e. more heterogeneous) multifractal structure (Fig. 9).

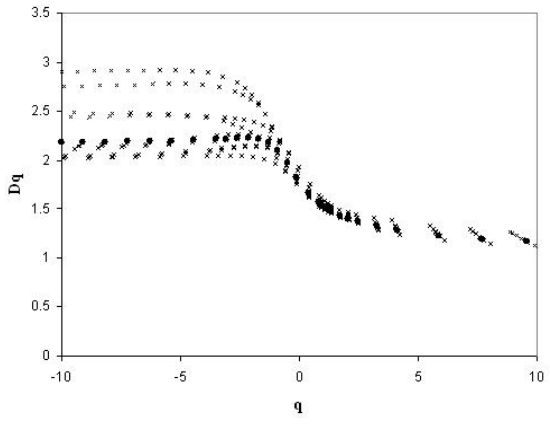

Fig. 7. The spectra of generalized fractal dimensions D_q for the spatial distribution of epicenters in the Alborz – Kopeh Dagh region. Symbols are shown in Fig. 3.

The maximum fractal dimensions $D_{-\infty}$ of about 2.18±0.33 and the minimum dimensions $D_{+\infty}$ of about 1.15±0.05 were calculated for the epicentral

distribution in the Alborz-Kopeh Dagh region (Table1).

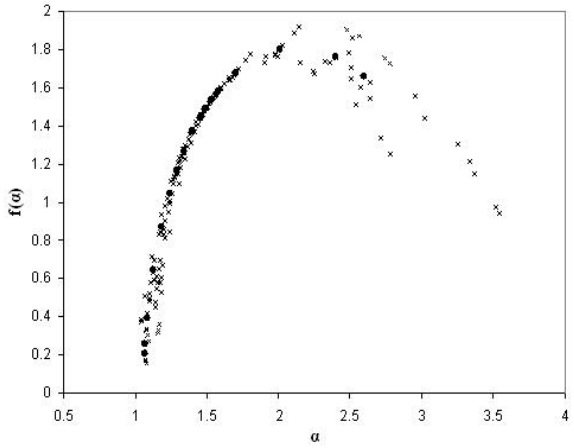

Fig. 8. The multifractal or singularity spectrum $f(\alpha_q)$ for the spatial distribution of epicenters in the Alborz-Kopeh Dagh region. Symbols are shown in Fig. 3.

The value of D_0 of about 1.82±0.05, D_1 about 1.53±0.03, and D_2 about 1.4±0.03 were calculated for the epicentral distribution (Table 1).

The multifractal parameters characterizing the $f(\alpha_q)$-spectrum of the epicentral distribution is given in Table 1. A value of α_0=2.01±0.07 was determined for the local fractal dimension related to the peak of $f(\alpha_q)$-spectrum. The values of w=2.2±0.44, Δ=1.2±0.25, and P_c =1.84±0.38 indicate that the epicentral distribution in the Alborz-Kopeh Dagh region has a multifractal structure with a relatively wider range of fractal exponents than the Zagros belt (Table 1).

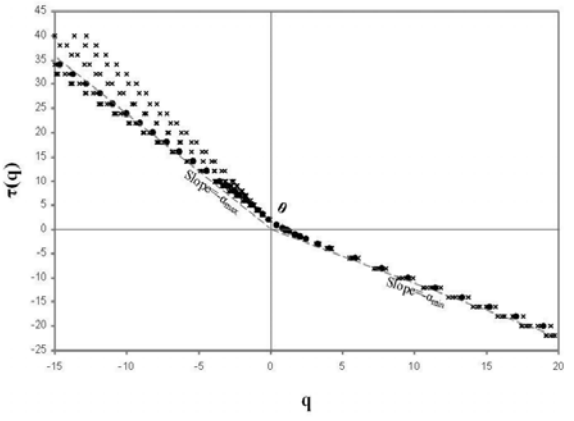

Fig. 9. The hierarchy of scaling exponents τ(q) or τ(q)-spectrum as a function of moment order q with the asymptotes (dashed lines) for the spatial distribution of epicenters in the Alborz-Kopeh Dagh region. In order to avoid the scatter-estimation errors for high values of q, the vertex θ is determined for the range of q between -4.0 and 4.0. Symbols are shown in Fig. 3.

In contrast to the Zagros belt, the parameters of steepness A=-0.7±0.07, and asymmetry B=0.13± 0.06 (right-skewed) indicate a gentle fall of $f(\alpha_q)$ spectrum with a slight positive skewness, characterized by a relative dominance of high-fractal exponents for the Alborz-Kopeh Dagh region.

Table 1. Multifractal parameters of the spatial distribution of epicenters in the Zagros and Alborz-Kopeh Dagh regions. With the standard error in parenthesis.

Parameters / Region	Zagros	Alborz-Kopeh Dagh
D_0	1.83 (± 0.03)	1.82 (± 0.05)
D_1	1.63 (± 0.02)	1.53 (± 0.03)
D_2	1.5 (± 0.01)	1.4 (± 0.03)
$D_{-\infty}$	2.29 (± 0.17)	2.18 (± 0.33)
$D_{+\infty}$	1.13 (± 0.01)	1.15(± 0.05)
α_0	1.92(± 0.06)	2.01 (± 0.07)
w	1.7(± 0.29)	2.2 (± 0.44)
Δ	0.93 (± 0.16)	1.2 (± 0.25)
P_c	1.32 (± 0.28)	1.84 (± 0.38)
A	-1.38(±0.04)	-0.70(± 0.07)
B	-0.12(±0.03)	+0.13 (± 0.06)
θ	170º	160º

5. Discussion and conclusions

The results of the studies carried out in this paper indicate that the generalized correlation integral functions $\left(\left\langle R_q \right\rangle\right)$ of the spatial distribution of earthquake epicenters in the Zagros and Alborz-Kopeh Dagh regions of Iran have multifractal structures. The middle portion of the $\left(\left\langle R_q \right\rangle\right)$ curve, i.e. for the Zagros in the distance range 20-100 km and for the Alborz-Kopeh Dagh in the distance range 20-130 km, shows linear or scale-invariant behaviour, indicating that the spatial patterns of seismicity in these regions have multifractal structures. The lower boundaries of the scaling ranges for the Zagros and Alborz-Kopeh Dagh are m=10 and 3, respectively, corresponding approximately to a distance of 20 km for both regions. This boundary was controlled by the location errors which are up to 15-20 km for the global earthquake catalogues used in this research. On the other hand, the upper cut-off for scaling range is m= 160 for the Zagros and m= 58 for the Alborz-Kopeh Dagh regions, respectively, that was controlled by box boundary effects and the size of the major seismogenic fault zones in these regions (Fig. 1). The variations of D_q for the spatial

distribution of earthquake epicenters in the Zagros and Alborz-Kopeh Dagh regions could be the result of different underlying dynamics that may be operating in these regions. In contrast to the Zagros region, the D_q spectrum for the Alborz-Kopeh Dagh has a gentle slope for q>0, i.e. saturate rapidly towards $D_{+\infty}$, while the convergence to the $D_{-\infty}$ is steep. This implies that the sparsely populated regions in the Alborz -Kopeh Dagh are more heterogeneous than those in the Zagros. The differences in the degree of heterogeneity within the multifractal distribution of earthquake epicenters in these regions are also confirmed by the relatively wider vertex of the $\tau_{(q)}$-spectrum of the Zagros with respect to the Alborz-Kopeh Dagh region. The results also indicate the multifractal seismicity patterns of both regions have asymmetrical distribution, resulting in the leaning of the $f(\alpha_q)$- α_q diagrams for both regions.

The relatively higher values of w, Δ, and P_c for the Alborz-Kopeh Dagh region indicate that the seismicity in this region has a rich or broad non-uniform (i.e. heterogeneous) multifractal structure denoted by a relative wide range of fractal exponents. This fact is also confirmed by the low value of steepness parameter A for the Alborz-Kopeh Dagh region. The asymmetry parameters B for the Zagros and Alborz-Kopeh Dagh regions indicate that the $f(\alpha_q)$ spectra of the regions were skewed but with differences in the direction of skewing, indicating strong weighted high fractal exponents in the $f(\alpha_q)$ spectrum of the Alborz-Kopeh Dagh region.

The analysis reveals that although the spatial distribution of earthquake epicenters in the Zagros and Alborz-Kopeh Dagh have multifractal structures, the seismicity of the Zagros region has a narrow or smooth multifractal (i.e. less heterogeneous fractal) structure. This fact may reflect the differences in physics and underlying structures of the seismotectonic processes in these regions. Furthermore, the estimated b-value for the Zagros and Alborz-Kopeh Dagh are 1.47±0.03 and 1.29±0.02, respectively. The most frequent explanation for the relatively high b-value in the Zagros belt is a weak lithosphere, incapable of sustaining high strain levels and a very heterogeneous stress system. Most earthquakes occur in such weak crusts, and their occurrence has often been related to the movements of small fault segments. The diffused seismicity with fewer larger earthquakes relative to smaller ones in the Zagros and relatively low level of seismicity with sporadic occurrence of strong destructive events in the Alborz-Kopeh Dagh confirm our findings.

The seismotectonic characteristics of the Zagros and Alborz-Kopeh Dagh regions are the result of recursive faulting and healing over a long period of geological times. The seismicity patterns in these regions were controlled by the tectonic stress field, and, at the same time the state of stress was changed by the occurrence of earthquakes. Multifractal analysis of spatial distribution of earthquake epicenters in the Zagros and Alborz-Kopeh Dagh regions shows dominant heterogeneous multifractal distribution of seismogenic fault zones. The intrinsic characteristic scales of seismogenic faults were probably related to the length of the lithospheric plate boundaries, lithospheric thickness, width of seismogenic belt, down dip width of the slab, and the topographic relief and/or isostatic anomalies within the lithospheric plates. The presence of multifractal structure in the seismicity pattern reveals the effect of a heterogeneous lithosphere, in which the heterogeneity occurs at different scales. Multifractal analysis of seismicity in the Zagros and Alborz-Kopeh Dagh regions is a useful tool in studying the physics and underlying structures of earthquake related phenomena. It is particularly useful for showing patterns in earthquake activity of a region that could not be discovered by any other means.

Acknowledgments

We thank M. Tohidi for her valuable comments. The skill of S. Farahi and Sh. Ansari in typing this manuscript from the original handwritten notes is appreciated. We are grateful to the Editor-in-Chief and reviewers of the Iranian Journal of Science and Technology for their suggestions. One of the authors (M. A.) thanks the Ministry of Sciences, Research and Technology and Golestan University for their financial support. This work was supported by the Center of Excellence for Environmental Geohazards, and the Research Council of Shiraz University.

References

[1] Bak, P., Tang, C. & Weisenfeld, K. (1987). Self-organized criticality: an explanation of 1/f noise. *Phys. Rev. Lett., 59*, 381-384.

[2] Bak, P. & Tang, C. (1989). Earthquakes as self-organized critical phenomena. *Journ. Geophys. Res., 94*, 15635-15637.

[3] Sadovskiy, M. A., Golubeva, T. V., Pisarenko, V. F. & Shnirman, M. G. (1985). Characteristic dimensions of rock and hierarchical properties of seismicity. *Phys. Solid Earth, 20*, 87-95

[4] Smalley, R. F., Chatelain, J. L., Turcotte, D. L. & Pre´vot, R. (1987). A fractal approach to the clustering of earthquakes: application to the seismicity of the New Hebrides. *Bull. Seism. Soc. Am., 77*, 1368-1381.

[5] Chen, K., Bak, P. & Obukhov, S. P. (1991). Self-organized criticality in a crack-propagation model of earthquakes. *Phys. Rev. A, 43*, 625-630.

[6] Evison, F. F. (2001). Long-range synoptic earthquake forecasting: an aim for the millennium. *Tectonophysics, 338*, 207-215.
[7] Goltz, C. (1997). *Fractal and Chaotic properties of earthquakes*. Berlin, Springer-Verlag, 178
[8] Guo, Z. Q. & Ogata, Y. (1997). Statistical relations between the parameters of aftershocks in time, space, and magnitude. *Journ. Geophys. Res., 102*, 2857-2873.
[9] Huang, J. & Turcotte, D. L. (1990). Are earthquakes an example of deterministic chaos?. *Geophy. Res. Lett., 17*, 223-226
[10] Kagan, Y. & Jackson, D. (1991). Long term earthquake clustering. *Geophy. Journ. Int., 104*, 117-133.
[11] Kagan, Y. & Knopoff, L. (1976). Statistical search for nonrandom features of seismicity of strong earthquakes. *Phys. Earth Planet Inter., 12*, 291- 318.
[12] Kagan, Y. & Knopoff, L. (1980). Spatial distribution of earthquakes: the two point correlation function. *Geophy. Journ. Roy. Astro. Soc., 62*, 303-320.
[13] Li, J., Chen, Y. & Mi, H. (2002). 1/f b temporal fluctuation: detecting scale-invariance properties of seismic activity in North China. *Chaos, Solitons and Fractals, 14*, 1487-1494.
[14] Ouchi, T. & Uekawa, T. (1986). Statistical analysis of the spatial distribution of earthquakes-Variation of the spatial distribution of earthquakes before and after large earthquakes. *Phys. Earth Planet Int., 44*, 211-225.
[15] Telesca, L., Cuomo, V., Lanfredi, M., Lapenna, V. & Macchiato, M. (1999). Investigating clustering structures in time-occurrence sequences of seismic events observed in the Irpinia-Basilicata Region (Southern Italy). *Fractals, 7*, 221-234.
[16] Telesca, L., Nikolitanga, I. & Vallianatos, F. (2006). Time-scaling analysis of southern Aegean seismicity. *Chaos, Solitons and Fractals, 28*, 361–366.
[17] Gutenberg, B. & Richter, C. F. (1954). *Seismicity of the Earth and Associated Phenomenon*. 2nd edition. Princeton, Princeton University Press, 310.
[18] Aki, K. (1981). A probabilistic synthesis of precursory phenomena. In: Simpson DW & Richards PG (ed) Earthquake prediction: *An international Rev. Am. Geophys. Union, Maurice Ewing Ser, 4*, 566-574.
[19] King. G. (1983). The accommodation of large strains in the upper lithosphere of the Earth and other solids by self-similar fault system. *Pure and Applied Geophysics, 121*, 761-815.
[20] Lei, X. & Kusunose, K. (1999). Fractal structure and characteristic scale in the distributions of earthquake epicenters, active faults, and rivers in Japan. *Geophys. Journ. Int., 139*, 754-762.
[21] Turcotte, D. L. (1986). Fractals and Fragmentation. *Journ. Geophys. Res., 91(B2)*, 1921-1926.
[22] Enescu, B., Ito, K., Radulian, M., Popescu, M. & Bazacliu, O. (2005). Multifractal and Chaotic Analysis of Vrancea (Romania) Intermediate-depth Earthquakes: Investigation of the Temporal Distribution of Events. *Pure and Applied Geophysics, 162*, 249-271.
[23] Geilikman, M. B., Golubeva, T. V. & Pisarenko, V. F. (1990). Multifractal patterns of seismicity. *Earth Planet Sci. Lett., 99*, 127-132.
[24] Hirata, T. & Imoto, M. (1991). Multifractal analysis of spatial distributions of microearthquake in the Kanto Region. *Gophys. Journ. Int., 107*, 155-162.
[25] Kiyashchenko, D., Smirnova, N., Troyan, V. & Vallianatos, F. (2003). Dynamics of multifractal and correlation characteristics of the spatio-temporal distribution of regional seismicity before the strong earthquakes. *Natural Hazards and Earth System Sciences, 3*, 285-298.
[26] Mittag, R. J. (2003). Fractal analysis of earthquake swarms of Vogtland/NW-Bohemia intraplate seismicity. *Journ. Geodynamics, 35*, 173-189.
[27] Telesca, L. & Lapenna, V. (2006). Measuring multifractality in seismic sequences. *Tectonophysics, 423*, 115-123.
[28] Sornette, A., Dubois, J., Cheminee, J. L. & Sornette, D. (1991). Are sequence of volcanic eruptions deterministically chaotic?. *Journ. Geophy. Res., 96*, 11931-11945.
[29] Aviles, C. A., Scholz, C. H. & Boatwright, J. (1987). Fractal analysis applied to characteristic segments of the San Andreas Fault. *Journ. Geophys. Res., 92*, 331-344.
[30] Zamani, A. & Agh-Atabai, M. (2009). Temporal characteristics of seismicity in the Alborz and Zagros regions of Iran, using a multifractal approach. *Journ. Geodynamics, 47*, 271-279.
[31] Zamani, A., Nedaei, M. & Boostani, R. (2009). Tectonic zoning of Iran based on self-organizing map. *Journ. of Applied Sciences* (In press).
[32] Zamani, A. & Hashemi, N. (2004). Computer-based self-organized tectonic zoning: a tentative pattern recognition for Iran. *Computer & Geosciences, 30*, 705-715.
[33] Badii, R. & Broggi, G. (1988). Measurement of the Dimension Spectrum f(α)-Fixed-mass Approach. *Phys. Lett. A, 131*(6), 339-343.
[34] Hirabayashi, T., Ito, K. & Yoshii, T. (1992). Multifractal Analysis of Earthquakes. *Pure and Applied Geophysics, 138*(4), 591–610.
[35] Engdahl, E. R., Jackson, J., Myers, S. C., Bergman, E. A. & Priestley, K. (2006). Relocation and assessment of seismicity in the Iran region. *Geophy. Journ. Int., 167*, 761-778.
[36] Jackson, J. A. & McKenzie, D. P. (1984). Active tectonics of the Alpine-Himalayan belt between Turkey and Pakistan. *Geophy. Journ. Roy Astron Soc. London, 77*, 185-264.
[37] Sepehr, M. & Cosgrove, J. W. (2005). Role of the Kazerun Fault Zone in the formation and deformation of the Zagros Fold-Thrust Belt, Iran. Tectonics, Doi, 1029/2004TC001725.
[38] Berberian, M. (1995). Master blind thrust faults hidden under the Zagros folds-active basement tectonics and surface morphotectonics. *Tectonophysics, 241*, 193-224.
[39] Sella, G. F., Dixon, T. H. & Mao, A. (2002). REVEL: a model for recent plate velocities from space geodesy. *Journ. Geophys. Res., Doi.*, 10.1029/2000JB00033.
[40] Tatar, M., Hatzfeld, D., Martinod, J., Walpersdorf, A., Ghafori-Ashtiany, M. & Chery, J. (2002). The present day deformation of the central Zagros from

GPS measurements. *Geophys. Res. Lett., Doi.*, 10.1029/2002/GL015427.
[41] Ni, J. & Barazangi, M. (1986). Seismotectonics of Zagros continental collision zone and a comparison with the Himalayas. *Journ. Geophy. Res., 91*(B8), 8205-8218.
[42] Jackson, J. (1980). Error in focal depth determination and the depth of seismicity in Iran and Turkey. *Geophy. Journ. Roy Astron Soc., 61*, 285-301.
[43] Jackson, J. A., Priestley, K., Allen, M. & Berberian, M. (2002). Active tectonic of the South Caspian Basin. *Geophys. Journ. Int., 148*, 214-245.
[44] Berberian, M. (1981). Active faulting and tectonics of Iran. In: Gupta HK, Delany FM (ed), Zagros Hindu Kush Himalaya Geodynamic Evolution Geodynamic Series, 3, Am. Geophys. Union, Washington, DC and Geol. Soc. Am., Boulder, CO, 33-69.
[45] Berberian, M. & King, G.C.P. (1981). Towards a paleogeography and tectonic evolution of Iran. *Can. Journ. Earth Sci., 18*(2), 210-285.
[46] Chandra, U. (1981). Focal mechanism solutions and their tectonic implications for the eastern Alpine-Himalayan region. In: Gupta HK, Delany FM (ed) Zagros Hindu Kush Himalaya Geodynamic Evolution, Geodynamic Series,3. Am. Geophy. Union, Washington, DC and Geol. Soc. Am., Boulder, CO, 243-271.
[47] Stöcklin, J. (1966). *Tectonics of Iran* (in Russian). Moscow, In: Geotektonika, 1, USSR Academy of Sciences, 3-21.
[48] Stöcklin, J. (1968). Structural history and tectonics of Iran: a review. *Bull Am. Assoc. Petrol. Geol., 52*, 1229-1258.
[49] Stöcklin, J. (1977). Structural correlation of the Alpine ranges between Iran and Central Asia. *Me´moire H series, Societé géologique de France, 8*, 335-353.
[50] Zamani, B., Angelier, J. & Zamani, A. (2008). State of stress induced by plate convergence and stress partitioning in northeastern Iran, as indicated by focal mechanisms of earthquakes. *Journ. Geodynamics, 45*, 120-132.
[51] Tchalenko, J. S. (1975). Seismicity and structure of the Kopet Dagh (Iran, U. S. S. R.). *Phil. Trans. R Soc. London Ser. A 278 A*, 1-28.
[52] Rustanovich, D. N. & Shirakova, E. I. (1964). Some results of a study of the Ashkabad earthquake of 1948. *Izv Akad Nauk USSR Ser. Geophiz.*, 1077-1080.
[53] Berberian, M. & Yeats, R. S. (1999). Patterns of historical earthquake rupture in the Iranian Plateau. *Bull Seismol. Soc. Am., 89*, 120-139.
[54] Ambraseys, N. N. & Melville, C. P. (1982). *A history of Persian earthquakes*. England, Cambridge University Press, Cambridge, 219.
[55] ISC (2008). International Seismological Centre, Newbury, Berkshire, United Kingdom.
[56] PDE (2008). Preliminary Determination of Epicenters. Monthly Listing, US Department of the Interior, Geol. Surv., National Earthquake Information Center, Denver, Colorado, USA.
[57] Aghanabati, A. (2004). *Geology of Iran (in Persian)*. Tehran, Geological Survey of Iran, 583.
[58] Wiemer, S. & Wyss, M. (2000). Minimum magnitude of completeness in earthquake catalogs: examples from Alaska, the Western United States, and Japan. *Bull Seism. Soc. Am., 90*, 859-69.
[59] Wiemer, S. (2001). A software package to analyze seismicity: ZMAP. *Seis. Res. Lett., 72*, 373-382.
[60] Berberian, M. (1979). Evaluation of the instrumental and relocated epicenters of Iranian earthquakes. *Geophy. Journ. Roy Astron Soc., 58*, 625-630.
[61] Sweeney, J. (1996). *Accuracy of Teleseismic Event Locations in the Middle East and North Africa*. Lawrence Livermore National Laboratory, UCRL-ID-125868.
[62] Kagan, Y. (2007). Earthquake spatial distribution: the correlation dimension. *Geophys. J. Int., 168*, 1175-1194.
[63] Halsey, T. C., Jensen, M. H., Kadanoff, L. P., Procaccia, I. & Shraiman, B. I. (1986). Fractal measures and their singularities: The characterization of strange sets. *Phys. Rev. A, 33*, 1141-1151.
[64] Goltz, C. (1996). Multifractal and entropic properties of landslides in Japan. *Geol. Rundsch, 85*, 71-84.
[65] Mandelbrot, B. B. (1974). Intermittent turbulence in self-similar cascades: divergence of high moments and dimensions of the carrier. *J. Fluid Mech., 62*, 331-358.
[66] Meneveau, C. & Sreenivasan, K. R., (1991). The multifractal nature of turbulent energy dissipation. *J. Fluid Mech., 224*, 429-484.
[67] Peitgen, H. O., Jürgens, H. & Saupe, D. (2004). *Chaos and Fractals: New frontiers of science*. 2nd edition, New York, Springer-Verlag, 864.
[68] Diego, J. M., Martinez-Gonzales, E., Sanz, J. L., Mollerach, S. & Mart, V. J. (1999). Partition function based analysis of cosmic microwave background maps. *Mon Not R Astron Soc., 360*, 427-436.
[69] Mandelbrot, B. B. (1989). Multifractal measures: especially for the geophysist. *Pure and Applied Geophysics, 131*, 5-42.
[70] Falconer, K. (2003). *Fractal Geometry. Mathematical foundation and applications*. 2nd edition, New York, Wiley, 366.
[71] Halsey, T. C. & Jensen, M. H. (1986). Spectra of scaling indices for fractal measures- theory and experiment. *Physica D, 23*, 112-117.
[72] Stanley, H. E. & Meakin, P. (1988). Multifractal phenomena in physics and chemistry. *Nature, 335*, 405-409.
[73] Frisch, U. & Parisi, G. (1985). Fully developed turbulence and intermittency. In: Ghil, M., Benzi, R., Parisi, G., Proceedings of the International School Physics "Enrico Fermi", LXXXVIII, Turbulence and Predictability of Geophysical Fluid Dynamics and Climate Dynamics. North Holland, Amsterdam, The Netherlands, 84.
[74] Chhabra, A. B., Mene Veau, C., Jensen, R. V. & Sreenivasan, K. R. (1989). Direct determination of the f(α) singularity spectrum and its application to fully developed turbulence. *Phys. Rev. A, 40*(9), 5284-5294.
[75] Wiemer, S. & Zúñiga, R. F. (1994). ZMAP-a software package to analyze seismicity, EOS, Transactions, Fall Meeting, AGU, 75, 456.
[76] Carbone, V. & Savaglio, S. (1996). Multifractal structure of Lyα clouds: an example with the spectrum of QSO 0055-26. *Monthly Not Roy Astron Soc., 282*, 868-872.

[77] Borda-de-Ague, L., Hubbell, S. P. & He, F. (2007). *Scaling biodiversity under neutrality*. In: Storch D, Mazquent P. A., Brown J. H. (Eds) Scaling Biodiversity, Cambridge University Press, 347-375.

[78] Grasberger, P. & Procaccica, I. (1983). Measuring the strangeness of attractors. *Physica D, 9*, 189-208.

[79] Kortas, L. (2005). Search for chaotic dynamics manifestation in multiscale seismicity. *Acta Geophy. Polonica, 53*(1), 47-74.

[80] Vicsek, T. (1993). *Fractal Growth Phenomena*. 2nd edition. Singapore, World Scientific, 240.

[81] Shimizu, Y., Thurner, S. & Ehrenberger, K. (2002). Multifractal spectra as a measure of complexity in human posture. *Fractals, 10*, 103-116.

[82] Tchalenko, J. S. & Braud, J. (1974). Seismicity and structure of Zagros (Iran): the Main Recent Fault between 338 and 358 N. *Philosophical Transactions of the Royal Society of London, 277* (1262), 1-25.

[83] Nerenberg, M. A. H. & Essex, C. (1990). Correlation dimension and systematic geometric effects. *Phys. Rev., A 42*, 7065-7074.

[84] Rydelek, P. A. & Sacks, I. S. (1989). Testing the completeness of earthquake catalogues and the hypothesis of self-similarity. *Nature, 337*, 251-253.

[85] Zamani, A. & Hashemi, N. (2000). A comparison between seismicity, topographic relief, and gravity anomalies of the Iranian plateau. *Tectonophysics, 327*, 25-36.

[86] Tavakoli, F., Walpersdorf, A., Authemayou, C., Nankali, H. R., Hatzfeld, D., Tatar, M., Djamour, Y., Nilforoushan, F. & Cotte, N. (2008). Distribution of the right-lateral strike–slip motion from the Main Recent Fault to the Kazerun Fault System (Zagros, Iran): Evidence from present-day GPS velocities. *Earth Planet Sci. Lett.* (In press).

[87] Vernant, Ph., Nilfroushan, F., Chery, J., Bayer, R., Djamour, Y., Masson, F., Ritz, J. F., Sedighi, M. & Tavakoli, F. (2004). Deciphering oblique shortening of central Alborz in Iran using geodetic data. *Earth Planet Sci. Lett., 223*, 177-185.